

## RESEARCH ARTICLE

# Ephemeral landform development following rapid coastal uplift in the southern orogen of Taiwan

Slawomir Jack Giletycz<sup>1</sup>  | Andrew Tien-Shun Lin<sup>1</sup> | Katsura Yamada<sup>2</sup> | Liang-Chi Wang<sup>3,4</sup> | Chih-Wei Chien<sup>5</sup>  | Jiann-Yuh Lou<sup>6</sup> | Neng-Wei Huang<sup>7</sup> | Che-Yung Ting<sup>7</sup> | Kuo-Wei Shih<sup>7</sup>

<sup>1</sup>Department of Earth Sciences, National Central University, Taoyuan City, Taiwan

<sup>2</sup>Department of Geology, Faculty of Science, Shinshu University, Nagano, Japan

<sup>3</sup>Department of Earth and Environmental Sciences, National Chung Cheng University, Chiayi County, Taiwan

<sup>4</sup>Environment and Disaster Monitoring Center, National Chung Cheng University, Chiayi County, Taiwan

<sup>5</sup>Exploration and Development Research Institute, CPC Corporation, Miaoli City, Taiwan

<sup>6</sup>Department of Marine Science, ROC Naval Academy, Kaohsiung City, Taiwan

<sup>7</sup>Sinotech Engineering Consultants, Ltd., Taipei City, Taiwan

## Correspondence

Andrew Tien-Shun Lin, Department of Earth Sciences, National Central University, 300 Jungda Road, Chungli, Taoyuan City, Taiwan.

Email: andrewl@ncu.edu.tw

## Funding information

Ministry of Science and Technology, Grant/Award Number: MOST 108-2116-M-008-002; Shinshu University

## Abstract

Newly emerged landscapes above sea level are characterized by rapidly evolving geomorphic systems where the initial fluvial pattern adapts to a former submarine topography. Such an early formed fluvial system establishes drainage basins and unstable landforms that characterize high topographic asymmetry which are prone to fast removal or reorganization. Transitional landscapes might form depositional systems as lakes or ponds that subsequently are incised, captured and incorporated into drainage basins. In this study we focus on the recently emerged Hengchun Peninsula to survey its paleoenvironment evolution. Three drillings performed in the Gangkou basin with fieldwork revealed several indicators that reconstructed stages of the landscape reorganization. The major finding shows an ephemeral large lake in the central part of the Hengchun Peninsula that was drained to the Pacific c. 6000 BP. The lake belonged to an ephemeral lakeland that was created after the emergence of the peninsula. Currently, several areas as relict landforms indicate this stage of topography evolution that through high rates of incision and subsequent captures, transforms into drainage basins. Furthermore, two drillings show brackish waters at the present estuary of the Gangkou basin. These two different paleoenvironments today build one system – Gangkou catchment. Long-term uplift rates show that a hanging wall of the Hengchun Fault plays a significant role in the creation of a lakeland by tilting the peninsula's surface. The tilt impacts on asymmetrical emergence of the peninsula and catchment development. Our study shows that a new geomorphic system might create depositional ephemeral landforms (lakes) that represent phases of early topography evolution after emergence above a sea level that are subjected to instantaneous rearrangement and evolves through large-scale phases before it reaches a topographic steady-state.

## KEYWORDS

emerging landscape, ephemeral lakes, new geomorphic system, southern Taiwan, topography rearrangement

## 1 | INTRODUCTION

Landscapes that have emerged above sea level are often characterized by ephemeral landforms, because they are built of submarine topography that has not been previously affected by surface erosional processes. In this study, we describe such a setting as a 'new

geomorphic system'. The exposure to subaerial conditions prompts rapid landscape reorganization. In this case, the topography is also characterized by an initial drainage system in which runoff accommodates to the former submarine topography until it evolves into a mature subaerial landscape. After subaerial emergence, the incipient topography is subjected to erosional processes dominated by fluvial

incision associated also with the formation of transient drainage systems (Figure 1). During this period, the drainage system is typically represented by an anomalous pattern, where drainage divides may not correlate to topographic highs (Hugget, 1988) as they are under constant migration or abrupt shifts due to incision and river captures (e.g. Dadson et al., 2003; Dahlquist et al. 2018; Giletycz et al., 2015; Hugget, 1988; Whipple et al., 2016). The emerging submarine topography may also contain enclosed topographic depressions where lakelands, ponds or marshes can form. If the hydrological budget sufficiently exceeds the runoff, these landforms might persist over millennia (Attal et al., 2008; Yang et al., 2011).

In this study we focus on the southernmost part of the Taiwan orogen, the Hengchun Peninsula, which has been emerging above sea level since the beginning of the Holocene (Figure 2), forming one of the youngest landscapes in Taiwan (Chen & Liu, 1993; Giletycz et al., 2015; Liew & Lin, 1987). This recent exposure of a submarine topography coupled with active tectonism (Giletycz et al., 2019; Huang et al., 1997) yields well-grounded conditions for rapid landscape rearrangement surveys. Additionally, the active Hengchun Fault at the western Hengchun Peninsula and a recent emergence of a lagoon at the western flank importantly impacts on the peninsula's landscape evolution (Giletycz et al., 2015).

Principally, we target a low-relief and low elevated terrain in the central and southern part of the Hengchun Peninsula, which is bounded by relict landforms such as ponds and lakes from the north

and southeast (Giletycz et al., 2015; Ramsey, 2006; Yang et al., 2011). We suggest that this area might preserve records of the larger scale initial geomorphic setting that represented topography after emergence above sea level. Using shallow drillings, pollen, foraminifera and ostracod stratigraphy as well as fieldwork surveys supported by DEMs (digital elevation models), we aim to reconstruct the temporal evolution of the paleoenvironments of this area of the Hengchun Peninsula. Then, we correlate the result with the long-term uplift rates from radiocarbon dating of marine terraces to build a larger scale evolutionary model and provide rates of the transformation from submarine to subaerial peninsula's topography.

## 2 | TECTONIC SETTING

Due to oblique collision between the Eurasian passive margin and Philippine Sea Plate, the uplift of Manila accretionary prism advances northward (e.g., Huang et al., 2006; Liu et al., 2001). This results in gradual shallowing of the submarine topography from the south towards the north and subsequent emergence of the accretionary prism above sea level in the southernmost part of Taiwan (Figure 2). The correlation of bathymetry data with surface topography of Taiwan shows that the Hengchun Ridge builds an offshore part of the Manila accretionary wedge-top, while to the north transforms into the onshore Hengchun Peninsula (Huang et al., 2006; Lin et al., 2009).

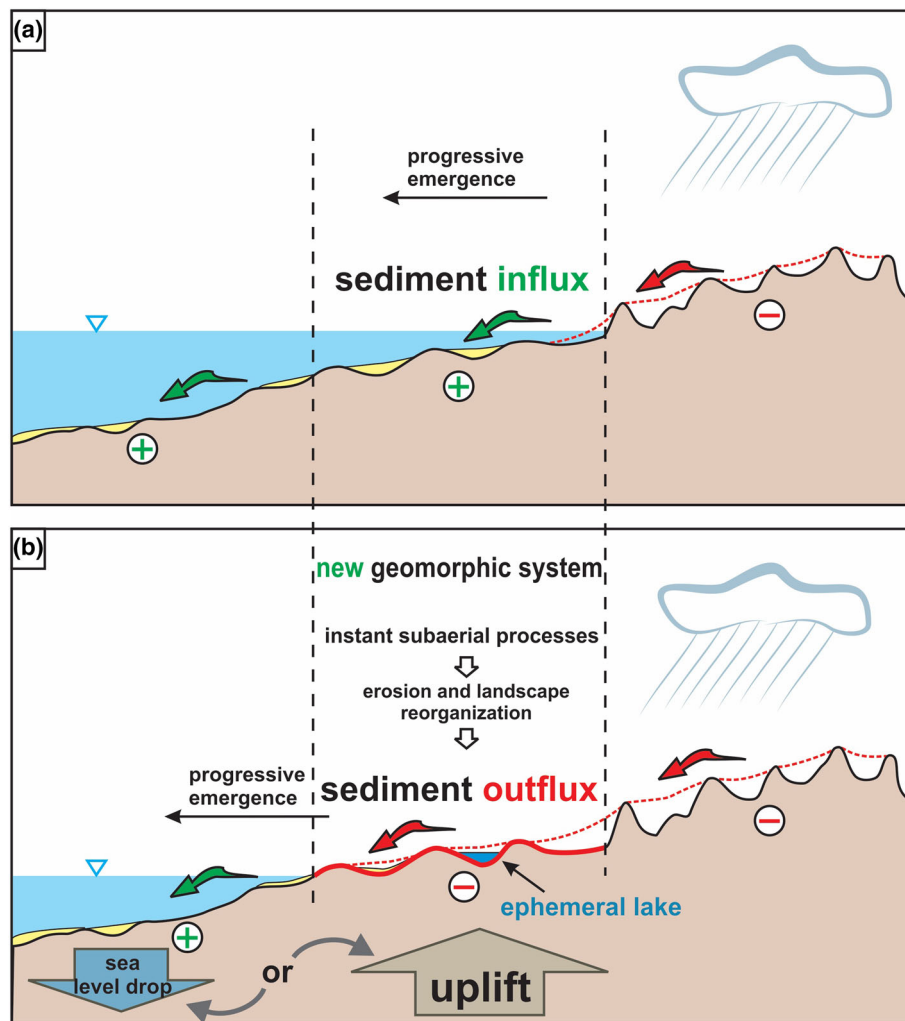


**FIGURE 1** Simplified conceptual model of a new geomorphic system before (a) and after (b) emergence above sea level. While the offshore area represents a depositional system dominated by sediment influx (a), the exposed topography to the surface processes transforms the geomorphic system to a sediment outflux domain (b). Instant initiation of the fluvial system coupled with precipitation that have more uniform impact on the entire surface lead to the landscape reorganization determined by diverse lithology, active tectonism, sea level fluctuations, and so forth. The transient submarine topography exposed to the fluvial processes also might tend to create ephemeral wetlands, lagoons, lakes or ponds. Plus (+) and minus (-) marks indicate sediment influx and outflux, respectively

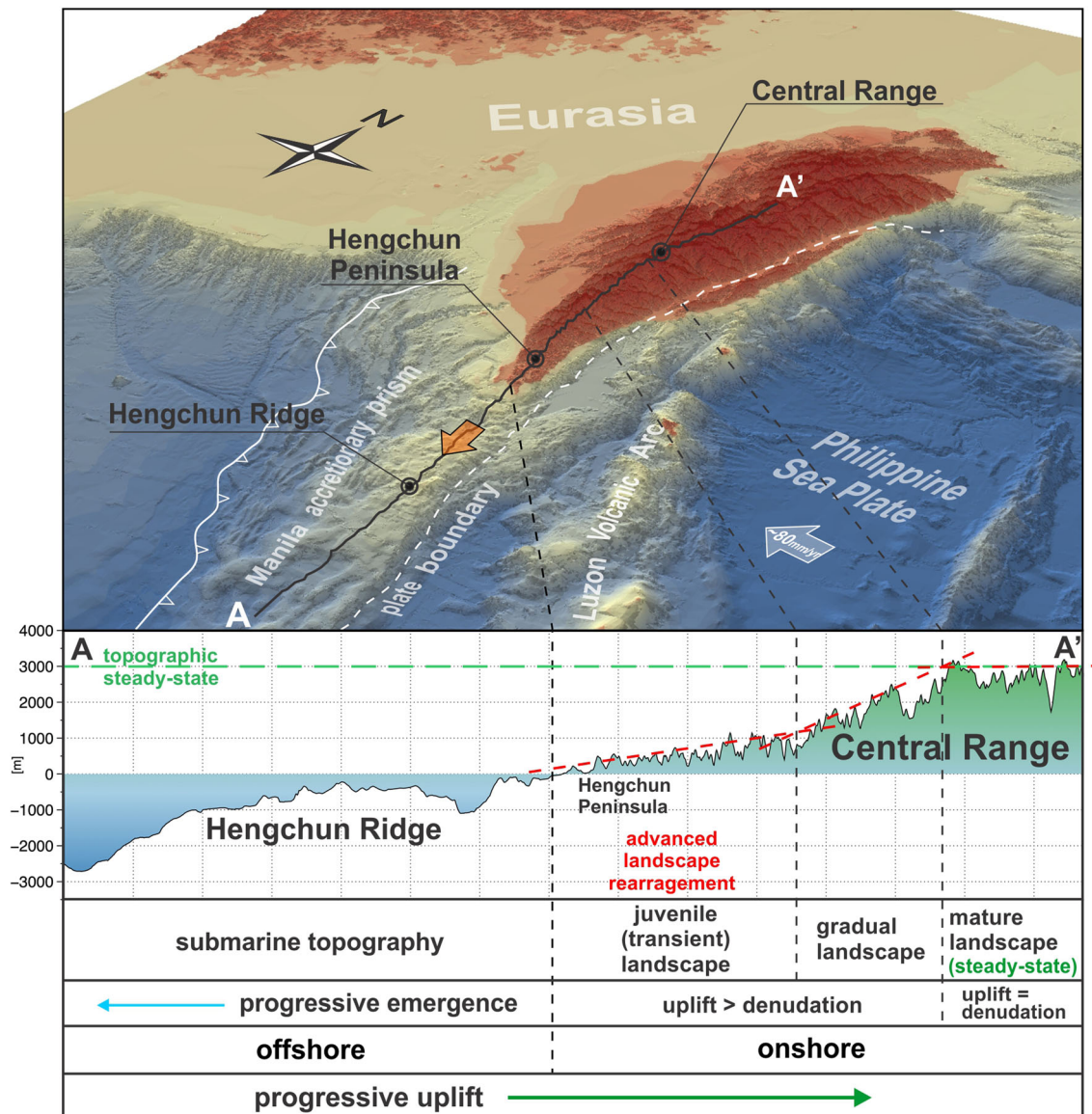


**FIGURE 2** Topography of the southern Taiwan and offshore areas. The oblique collision between Eurasia passive continental margin and the Luzon arc leads to a progressive emergence of the island towards the south. The bathymetric map shows a continuation of the topography gradually descending into the South China Sea down to over 2000 m. The white arrow indicates the collision direction, the orange arrow shows the direction of the emergence of Taiwan orogen. The topographic profile below, shows four stages of the topographic evolution of southern Taiwan. From the right, the Hengchun Ridge represents the submarine topography (i), while the newly emerged Hengchun Peninsula is under pluvial surface processes and is characterized by landscape reorganization (ii). Further north, in the southern Central Range the elevation of the topography gradually increases as a ‘gradual landscape’ (iii) (Hugget, 1988) and finally at about 2800–3000 m approaches topographic steady-state (iv) (Whipple, 2001; Ramsey et al., 2007; Stolar et al., 2007)

Several sets of marine terraces dispersed across the Hengchun Peninsula indicate a recent exposure of the topography to subaerial conditions (Chen & Liu, 1993; Liew & Lin, 1987). The marine terraces outcrop at various places along hanging and footwall of the Hengchun Fault, also along the emerged eastern coast of the peninsula, giving broad evidence of the surface uplift pattern across the peninsula. As a result, the Hengchun Peninsula represents the most recently emerged part of the Manila accretionary ridge and therefore, the most juvenile landscape of southern Taiwan. From here, the maturity of the Taiwan topography increases northward into the Central Range through a ‘gradual landscape’ (Hugget, 1988), which depicts conditions where uplift dominates over denudation. Finally, the landscape approaches a topographic steady-state equilibrium that is estimated in Taiwan at

about 3000 m above sea level (Figure 2) (Stolar et al., 2007; Whipple, 2001).

### 3 | GEOMORPHIC SETTING

The Hengchun Peninsula is characterized by a highly asymmetrical drainage system, while the main drainage divide in the southern Central Range represents a nearly symmetrical trend (Figure 3). In the northern peninsula the main drainage divide sharply bends towards the eastern coast. Here, at the upstream of the Fengkang basin, the distance of the main drainage divide to the eastern coast is less than 3.5 km, while to the western coast exceeds 17 km (Figure 3). This is

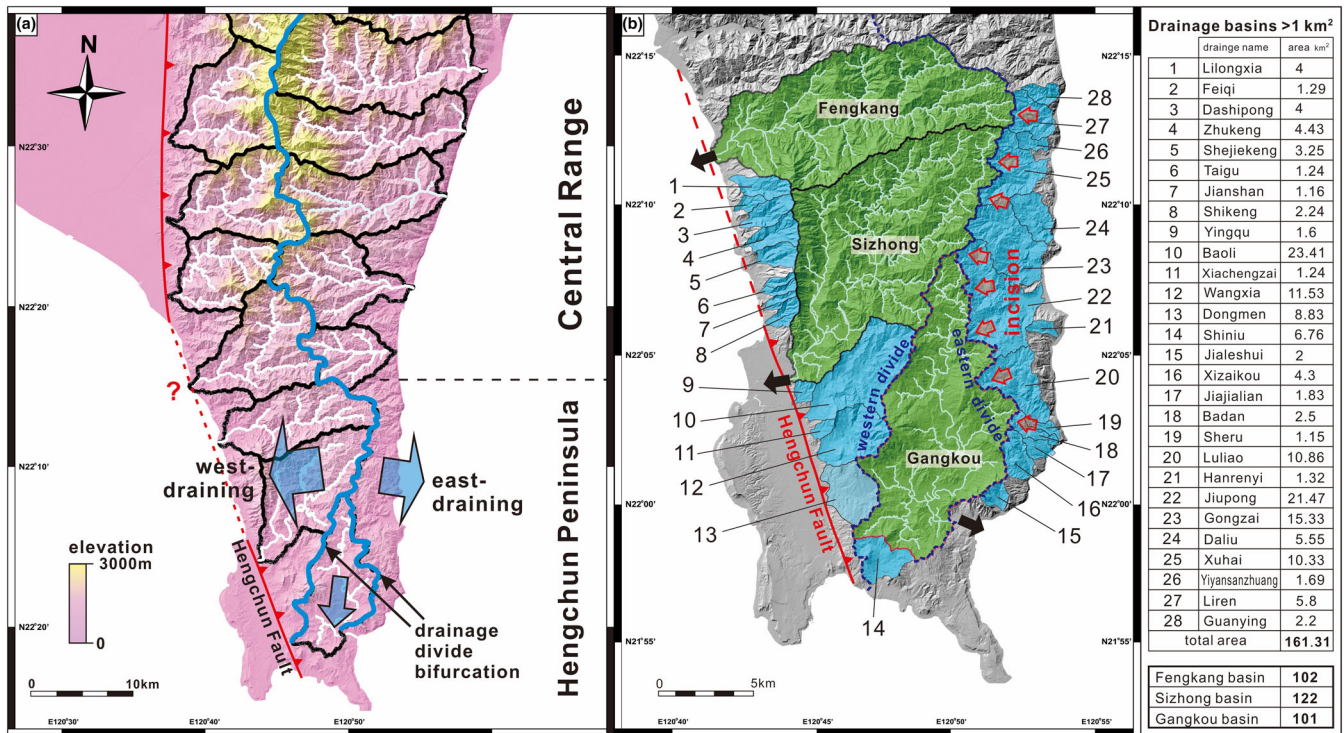


**FIGURE 3** (a) Drainage system of the southern Taiwan. The drainage divide is marked by thick blue line. Note, (x) the drainage divide bends toward the eastern coast while descending into Hengchun Peninsula, and (xx) the asymmetrical pattern of the drainage basins of the Hengchun Peninsula. Also, the drainage divide bifurcates at the south end of the peninsula ‘trapping’ the Gangkou basin in between. (b) Drainage system of the Hengchun Peninsula. Three major basins (Fengkang, Sizhong and Gangkou) cover over 320 km<sup>2</sup>, leaving less than a half of the peninsula’s surface to the other 28 small drainage basins mostly at the eastern side. The advanced incision from the east progressively capture the west draining basins (Ramsey, 2006; Giletycz et al., 2015). Black arrows indicate outlets of the three basins, which predominantly drain the peninsula’s surface

because two large drainage basins (Fengkang and Sizhong) cover almost the entire area of the northern peninsula and they drain to the western coast. Further to the south, the main drainage divide bifurcates trapping the Gangkou drainage basin in between, which is built of a 1-to-5 km wide low-relief area (Figure 4). This low-relief is progressively consumed by advancing incision and capture points from the eastern coast to the benefit of the 14 smaller drainage basins draining to the east (Figure 3b) (Giletycz et al., 2015; Ramsey, 2006). This results in the east bifurcation progressively migrating westward. Presumably, the eastern bifurcation will disappear and the main drainage divide will shift to the western bifurcation, with large drainage basins draining to the east. The western bifurcation separates the Fengkang and Sizhong basins from the Gangkou drainage basin. It runs obliquely across the central peninsula from northeast to southwest and finally, in the south, it reaches a hanging wall of the Hengchun Fault.

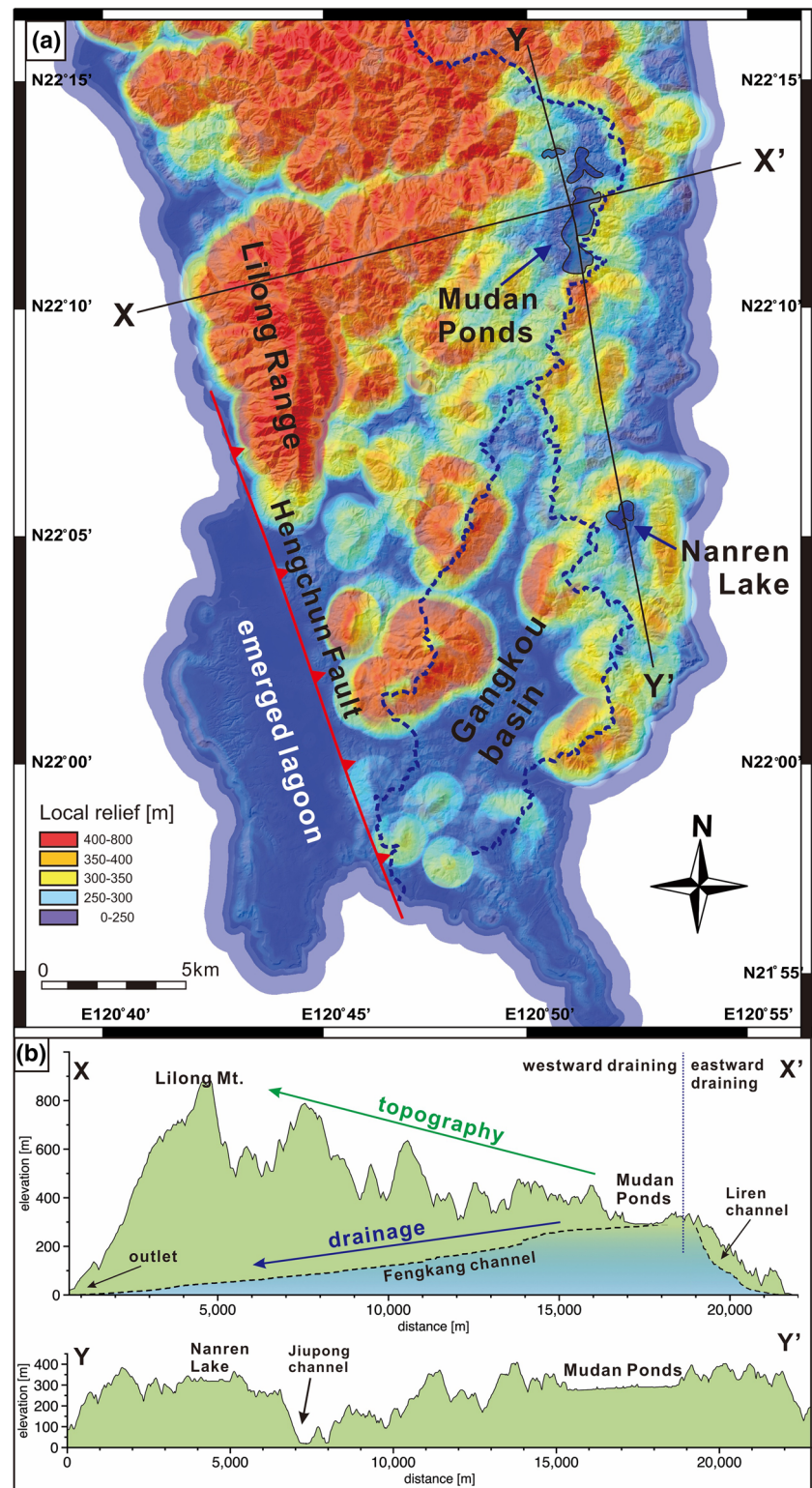
There are three major drainage basins in the Hengchun Peninsula: Fengkang, Sizhong and Gangkou, draining towards the west, southwest and south, respectively. Their combined area of over 320 km<sup>2</sup> drains most of the peninsula’s surface. Some 28 smaller basins drain about 33% of the peninsula’s surface with 14 of these draining to the east (Figure 3b). In the upper reaches of the Fengkang and Sizhong basins, low-relief, low-elevation areas of the Mudan Ponds are comprised of lacustrine deposits, which based on pollen and radiocarbon dating have yielded ages of over 21,000 years (Yang et al., 2011) (Figure 4). These Mudan Ponds are a relict landform of a lakeland of an older stage of the landscape evolution of the Hengchun Peninsula

(Giletycz et al., 2015). It also comprises the main drainage divide of the peninsula’s system. The progressive incision also simultaneously erodes Mudan Ponds, which prompts the eastern drainage divide to migrate westward (Figure 3b). The other relict of the former low-relief landscape is Nanren lake approximately 13 km to the south of the Mudan Ponds (Figure 4). The lake is located at the same elevation as the Mudan Ponds therefore it is believed that the area indicates the same paleoenvironment of the low-relief topography after the emergence of the peninsula (Figure 4b, profile Y–Y’).

Hengchun Peninsula’s topography however, represents a markedly contrasting pattern to the drainage system. The Lilong Range builds the highest topography and the highest relief landform of the peninsula, yet it is located downstream of the Fengkang and Sizhong basins (Figure 4b, profile X–X’). At the same time, the upstreams of the basins constitute the low-relief Mudan Ponds, and their elevations are one-third of the Lilong Range. This leads to a peculiar topographic inversion where sources of the Sizhong and Fengkang Rivers are in the low-relief areas with an elevation not surpassing 300 m above sea level, and flow towards the high-relief and high-elevated topography of over 1000 m (Figure 4b). This confirms that the main drainage divide does not correlate to the highest topography and is decoupled for about 13 km, which is two-thirds of the width of the peninsula.

The latitudinal east-to-west increase of the topography indicates asymmetric uplift rates that are linked to activity of the Hengchun Fault (Giletycz et al., 2017). To the southwest of the Lilong Range, an emerged lagoon built of Holocene sediments (Cheng & Huang, 1975;

**FIGURE 4** (a) Local relief map of the Hengchun Peninsula built on  $5\text{ m} \times 5\text{ m}$  digital elevation model (DEM), by  $5\text{ km}$  diameter circular sliding window with the mean value of the relief presented in the centre of the grid (see also profile later). Note, in the north, the lowest local relief areas are located at the eastern coast, while the highest relief appears at the western flank (Lilong Range). This shows that the highest topography does not correspond to the main drainage divide which is located at the eastern side of Mudan Ponds – one of the lowest-relief areas in the peninsula (b). (b) The profile shows asymmetrical topography of the Hengchun Peninsula where the main drainage divide does not correspond to the highest topography. As a result, main drainage divide crosses the lowest-relief (Mudan Ponds) from which two major drainage basins drain to the west (Fengkang channel profile in blue for comparison to the topography) towards the highest reliefs of the peninsula



Chen & Liu, 1993; Liew & Lin, 1987) also indicates westward expansion of the peninsula's surface (Figure 3b).

## 4 | METHODOLOGY

### 4.1 | Shallow drilling in Gangkou estuary

Three shallow boreholes were drilled in the lower reaches of the Gangkou basin by Sinotech Engineering Consultants, Ltd, Taiwan

(Figure 5). Two of them (KKC-01 and KKC-09) were located in the river's estuary, and one (KKC-13) in the inner part of the basin. The boreholes reached depths of 20, 18 and 16 m, respectively. The locations of the drilling sites were chosen: (1) to investigate paleoenvironmental conditions of the downstream area of the Gangkou basin, and (2) to determine whether or not the estuary might contain a record of a former main drainage divide and a potential capture point as reported in the northern areas in previous studies (Giletycz et al., 2015; Ramsey, 2006). The cores were stored at the Department of Earth Sciences, National Central University, Taiwan,

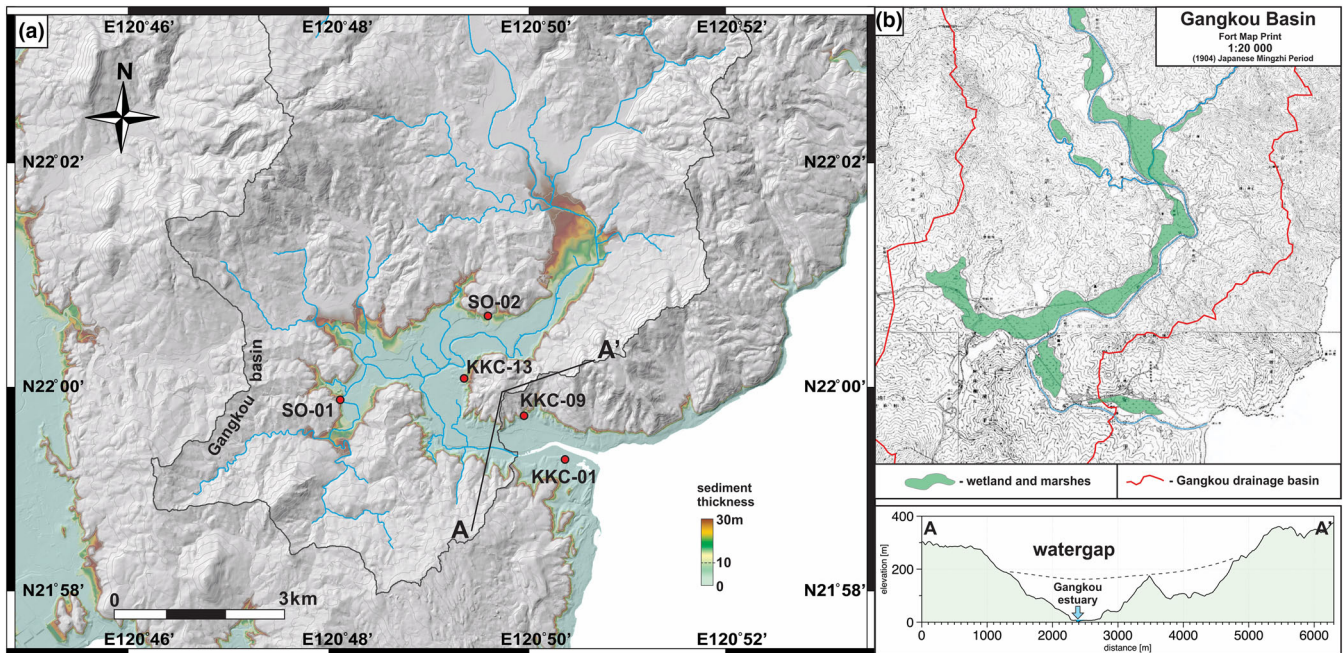


**FIGURE 5** (a) A 5-m digital elevation model (DEM) of the central and downstream of the Gangkou basin with drilling sites locations and outcrops that shows dark lacustrine mud deposits surveyed in this study. The colour bar represents a possible thickness of the lacustrine mud extrapolated on the DEM from the outcrop SO-01 (since we do not have any indications of lake depth, we adopt the highest elevation of the sediment at SO-01 outcrop to simulate the lake area). The A–A' profile across the Gangkou estuary shows a water gap through which the basin drains into the Pacific (profile down right). (b) Map of the Gangkou basin from 'Japanese Period' (1904) showing that still in the beginning of the 20th century the area represented wetlands and marshes (in green), possibly relicts of the former Manzhou Lake. In later years the marshes were dried for farming purposes

where lithological descriptions and core density profiles were carried out by the Sedimentology and Basin Research Group. The cores were then sent to the Naval Academy, Taiwan for multi-sensor core logger (MSCL) scanning (supplementary data is available at a public repository, see later). After the lithological description, samples were taken for pollen, diatom, foraminifera and ostracods determination as well as radiocarbon dating.

#### 4.1.1 | Pollen analyses

The samples for pollen analyses were collected from darkish mud in all three cores. These were sent to the Paleoenvironmental Research Laboratory at National Chung Cheng University, Taiwan. For each 1 cm<sup>3</sup> wet sample, a known content of fern (*Lycopodium*) spore ingot (each grain contains about 10,680 spores) and 5 ml 10% hydrochloric acid was added. After removing the waste liquid by centrifugation, 5 ml of 48% hydrofluoric acid was added and left for one week. After that time, the waste liquid was removed by three sessions of centrifugation (each 3000 rpm for 5 min). The organics were removed using the acetic acid method and concentrated by an ultrasonic bath on a nylon sieve of 10 μm mesh size. The pollen concentrate was mounted with glycerin jelly for microscopic examination. Pollen and spore counts were made using an Olympus BH-2 optical microscope. Each sample contained 100–150 pollen and spores (without additional *Lycopodium* spores).

The samples with low pollen preservation, less than 100 pollen and spores, were excluded from analysis and discussion. The formula for calculating the pollen content is as follows:

$$\text{pollen concentration} = \frac{\text{known quantity of } Lycopodium \text{ spore tablet added before chemical treatment}}{\text{total pollen grain counts}}$$

Pollen represents a male gamete of the seed plant and it is the most commonly used microfossil in reconstructing paleoenvironmental and climate studies as lakes, lagoons, interglacial and glacial transition (Anderson et al., 2014). Since the pollen wall is composed of acid-resistant strong alkali-sporopollenin, a large amount of pollen fossil is usually preserved in a sedimentary environment. By analysing the composition of the sporopollenin in sediments, we are able to reconstruct the changes in the composition of the surrounding vegetation and estimate a quantity of plants. Also, extreme environmental events such as heavy rainfalls or landslides can be depicted by abnormal changes in pollen compositions (Wang et al., 2015, 2019).

#### 4.1.2 | Foraminifera analyses

The foraminifera analysis was carried out by two laboratories: Sedimentary and Basin Research Group, Department of Earth Sciences at National Central University, Taiwan and Department of Earth Sciences at National Cheng-Kung University, Taiwan. Ten samples were collected from cores KKC-01, KKC-09 and KKC-13. The samples were dried in an oven for over 72 h then sieved in 63 and 125 μm sieves with clean water. The sediment inside foraminifera shells was washed out by 1 to 2 s shocks in an ultrasonic cleaner. The samples were dried again in the oven and sieved in 150 μm woven wire mesh sieve without water. The microfossils were picked out by brush and needle under an optical microscope and photographed by FEI Quanta 250 FEG scanning electron microscope.

The microfossil foraminifera mainly represent planktonic or benthic marine protozoa organisms that possess a shell, which due to their biodiversity and complex morphology is widely used for biostratigraphy and paleoenvironmental surveys as climate proxy, coastal environments, etc. Their assemblage can also be used for interpretation of marine sedimentary strata.

#### 4.1.3 | Ostracod analyses

Nineteen samples were taken from cores KKC-01, KKC-09 and KKC-13; six, two, and eleven, respectively. These were analysed at the Department of Geology, Faculty of Science, Shinshu University, Japan. Briefly, 1 cm thick mud was taken from each sample horizon. The samples were washed through 63  $\mu\text{m}$  mesh and then dried in an oven. Using a sample splitter, the residual sediment was divided into an adequate sample containing more than 200 ostracod specimens. All ostracod specimens were picked from the sample and identified under a binocular microscope and then photographed.

The ostracods, known as ‘seed shrimps’, are crustaceans often of 0.3 to 1 mm in size. They represent widespread arthropods, that due to easy preservation of their bivalve carapaces and abundance in marine strata are useful for paleoenvironment surveys including coastal and estuarine areas (Hong et al., 2019; Tanaka et al., 2019; Wang & Zhao, 1985; Whatley & Zhao, 1987; Zhao & Wang, 1988).

#### 4.1.4 | Radiocarbon dating

Six samples for radiocarbon dating from the three cores KKC-01, KKC-09 and KKC-13 (three, one and two, respectively) were sent to

Beta Analytic Laboratory, Miami, FL, USA. The samples were taken from dark-grey fine mud deposit (Figure 6). Five wood pieces were picked from KKC-01 (7.75, 10.61 and 15.81 m), KKC-09 (10.06 m) and KKC-13 (14.68 m), and one was taken from a log of a possible fallen tree (KKC-01, 10.61 m). The sample from KKC-13 (10.74 m) is organic sediment. The gathering of samples was performed under the strict chain of custody and quality control under ISO/IEC 17025:2005 Testing Accreditation PJLA #59423 accreditation protocols. The results were calibrated to calendar years (cal BC/AD) and calibrated radiocarbon years (cal BP). The calibration was calculated using the database associated with the 2013 INTCAL program. Conventional radiocarbon ages and uncertainties were rounded to the nearest 10 years per conventions of the 1977 International Radiocarbon Conference. When counting, statistics produced uncertainties lower than  $\pm 30$  years, a conservative  $\pm 30$  BP was cited for the result.

#### 4.2 | Fieldwork, digital elevation model surveys and active tectonism

Fieldwork was carried out between October 2017 and January 2019. It focused on the Gangkou drainage basin, its estuary, and along the east coast of the Hengchun Peninsula. The main target was to map and study possible relict landforms in order to place constraints on the history of drainage system reorganization and the paleoenvironment changes in the newly emerged geomorphic system. In particular, we looked for indicators of fluvial characteristics that could provide evidence of advancing river incision from the eastern basins that led to the main drainage divide migrating westward. The fieldwork and geological mapping were supported by a 5 m  $\times$  5 m resolution DEM provided by the ASO Forestry Bureau, Taiwan. For two-dimensional

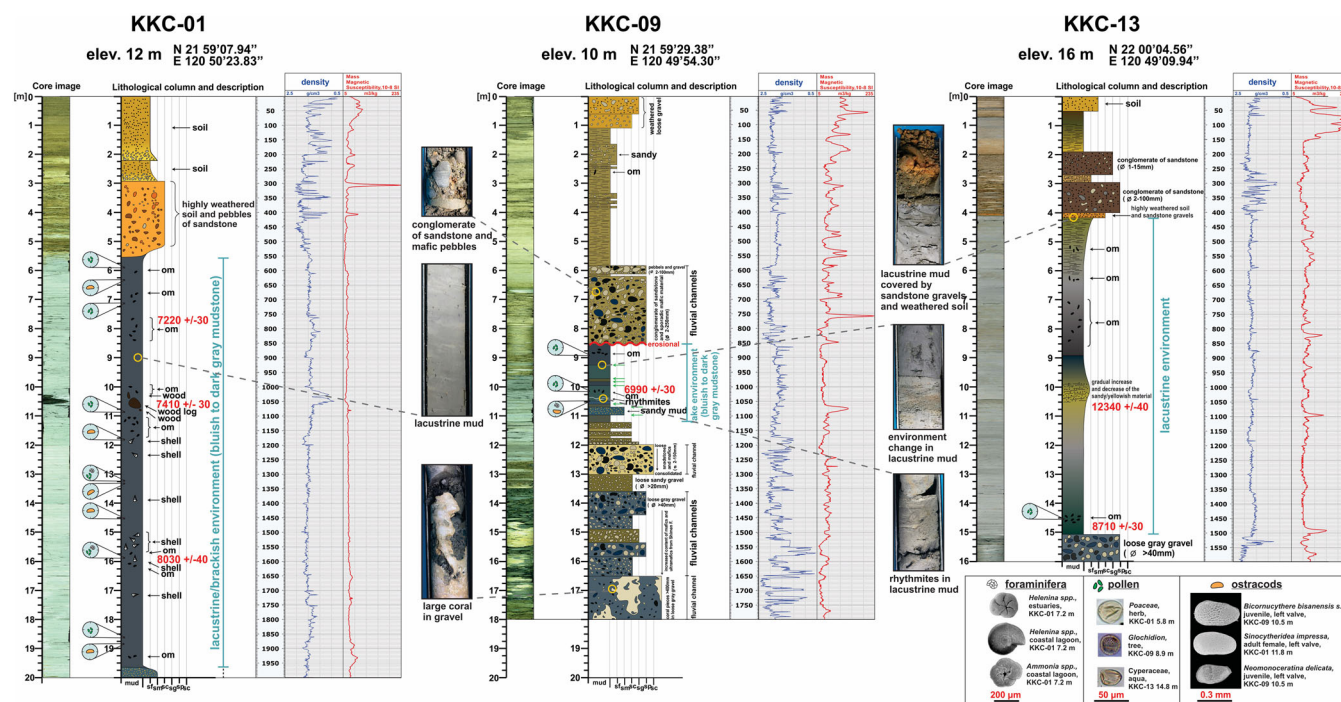


**FIGURE 6** Sedimentological core description with density and MMS (mass magnetic susceptibility) plots. Note, the MMS corresponds to the dark lacustrine or brackish waters sediment. Photographs show several characteristic horizons discussed in details in the text. Three symbols of pollen, ostracodes and foraminifera show the location of the specimens found in the cores and surveyed to reconstruct the paleoenvironment in the downstream of the Gangkou basin. Radiocarbon dating marked in red

(2D) and three-dimensional (3D) relief mapping a 5 km diameter circular sliding window with the mean value of the relief presented in the centre of the grid were used. The same digital model was utilized for a ‘lake simulation’ in the Gangkou basin.

The field investigation and environment reconstruction from the three boreholes were coupled with uplift rates of the Hengchun Peninsula from radiocarbon dating of marine terraces from previous studies (Cheng & Huang, 1975; Chen et al., 2014; Liew & Lin, 1987), also the long-term slip rate of the Hengchun Fault was estimated for the topographic deformation pattern. The results were correlated to data of fluvial characteristics or changes to deliver a reorganization model of the peninsula’s topography as a new geomorphic transient system.

## 5 | RESULTS

All three cores (KKC-01, KKC-09 and KKC-13) from the Gangkou drainage basin contain a layer of well-sorted, dark blue to dark grey fine material interpreted to have been deposited in a lacustrine or brackish environment (Figure 6) (full data results available at: [https://figshare.com/articles/dataset/data\\_giletycz\\_et\\_al\\_zip/12965276](https://figshare.com/articles/dataset/data_giletycz_et_al_zip/12965276), data openly available in a public repository that does not issue DOIs). The column of lacustrine or brackish sequence from KKC-01 and KKC-13 is bounded by progressive increase of coarse sediments, which indicates a calm period during the beginning and extinction of the waterbody. The KKC-09 core however, exposes a highly erosional contact enclosing poorly sorted sediments with pebbles, coarse sands or broken corals. Low values of mass magnetic susceptibility (MMS) and low density of the sediment along the three core columns

correlate to the dark layers of fine mud (Figure 6). All three cores show the same age interval from 8700 yr BP to over 6100 yr BP from the lower boundary to the top, respectively. We determine an approximate extinction of the lacustrine deposits around 6000 yr BP. In core KKC-13 however, coarse-grained sediments with organic matters at 10.15 m depth yielded an anomalous age of 12,340 yr BP; much older than the underlying sediments which yield an age of  $8710 \pm 30$  yr BP at 14.68 m depth. This might indicate that higher energy fluvial deposits, due to extreme events such as typhoons, monsoons or earthquakes, led to local landslide transported deposits from upper parts of the basin and were injected into the lake. No diatom fossils were found in any sample of any KKC cores.

### 5.1 | Pollen results

Three cores and two outcrops from the lower parts of the Gangkou basin and its estuary contain abundant organic matter, mostly wood pieces. Optical microscope analyses show also a large abundance of grass seeds, grass stems and other organic matter as small twigs or animal residues. In core KKC-01, we have also located a large log that we have interpreted as a fallen tree (at 10.5 m depth). Evidence of good pollen preservation aided comprehensive depositional environment reconstruction of the area.

In the core KKC-01 at the depth of 18.60 m the pollen concentration yielded 5406 pollen spores/cm<sup>3</sup>. The arboreal pollen (AP) content of the sample reached 7%. The dominant AP represented medium- and low-altitude forest with species such as *Alnus* (2%) and *Castanopsis* (2%). Non-arboreal pollen (NAP) is dominated by Cyperaceae (73%) and Poaceae (17%) (Figure 7). At the depth of 15.80 m the

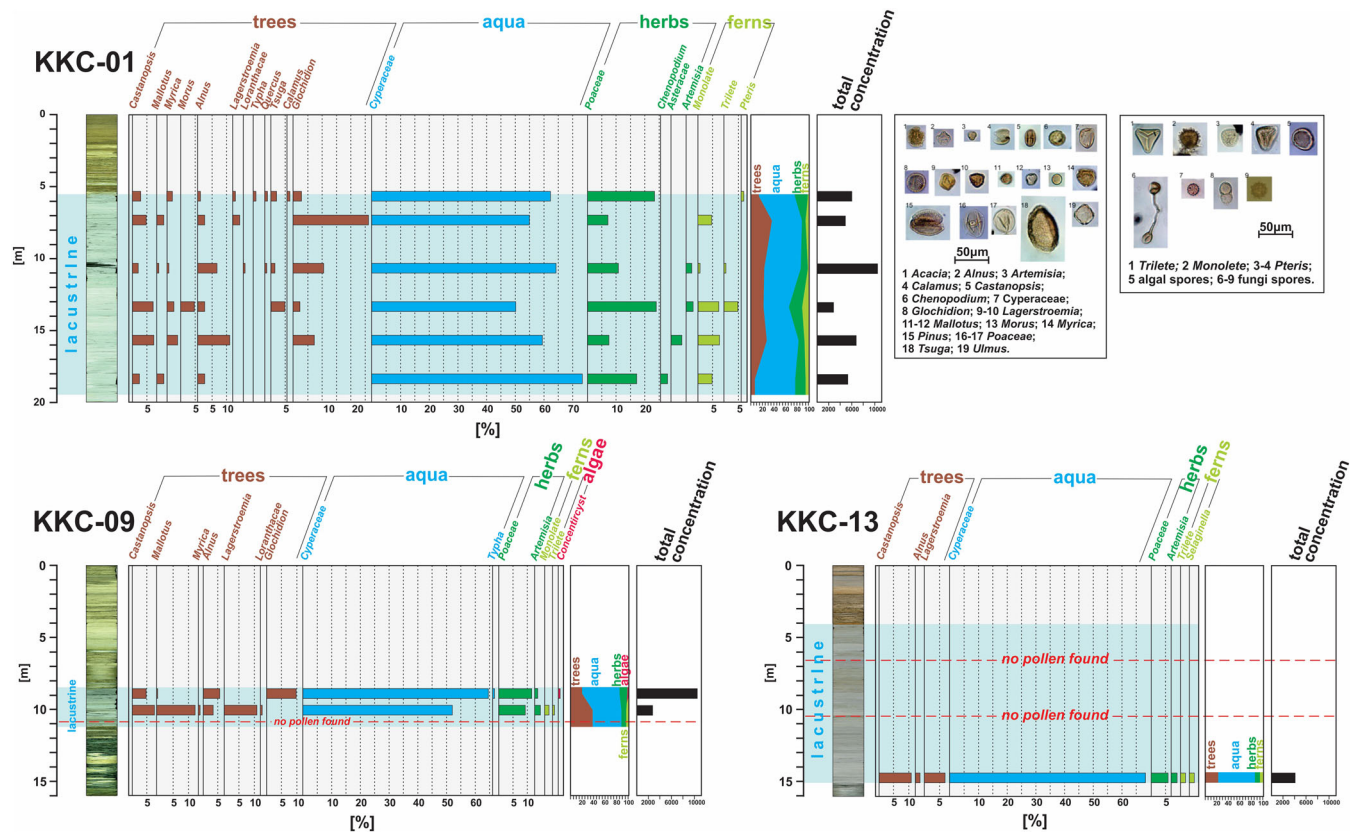


**FIGURE 7** Pollen data from the three cores KKC-01, KKC-09 and KKC-13. Large concentration of pollen was found in KKC-01. All three cores, show wetlands or lakes in vicinity of low-altitude forest

pollen concentration was 6706 pollen spores/cm<sup>3</sup>. The woody plant pollen content of the sample was 30%. The dominant AP is *Alnus* (11%), *Castanopsis* (7%) and *Glochidion* (7%). NAP was dominated by Cyperaceae (59%), which contains large amounts of other organic debris. A sample from 13.2 m showed a relatively low pollen concentration of 2857 pollen/cm<sup>3</sup> with AP content of 24%, and the main AP is low-altitude forest species such as *Castanopsis* (7%). NAP was dominated by Cyperaceae (50%), and Poaceae (24%), while fern spores make up to 12%. At the depth of 10.8 m the pollen concentration is 10,824 pollen spores/cm<sup>3</sup>. The AP content of the sample was 23%. The dominant AP are medium- and low-altitude forest species such as *Glochidion* (11%) and *Alnus* (7%). The NAP was dominated by Cyperaceae (64%) and Poaceae (10%). The sample from 7.20 m yielded pollen concentration of 4823 pollen spores/cm<sup>3</sup>. The AP content of the sample reached 38%, and the main dominant AP is low-altitude forest species such as *Glochidion* (26%) and *Castanopsis* (5%). NAP was dominated by Cyperaceae (55%). At 5.80 m depth, the pollen concentration yielded 6011 pollen spores/cm<sup>3</sup>. The AP content of the sample showed 14% with the dominant AP representing low-altitude forest species such as *Glochidion* (3%) and *Castanopsis* (3%). NAP was dominated by Cyperaceae (62%) and Poaceae (23%).

Three samples from KKC-09 were analysed from horizons of 8.9, 10.1 and 10.8 m, in which at 10.8 m no pollen was found (Figure 7). However, 10.1 m yielded relatively low pollen concentration of 2814 pollen spores/cm<sup>3</sup>. The AP content of the sample showed 39%, and the dominant AP represents low-altitude forest species such as *Mallotus* (13%) and *Lagerstroemia* (12%). NAP was dominated by Cyperaceae (52%) and Poaceae (9%) with domination of organic debris in the sediment. The sample from 8.9 m yielded a very high

pollen concentration of 11,348 pollen spores/cm<sup>3</sup>. The AP content of the sample reached 22%, where the main AP content represented low-altitude forest species such as *Glochidion* (10%). Wetland pollen was dominated by Cyperaceae (64%) and terrestrial herb represented by Poaceae (12%), which contained algal spores. No pollen at 10.8 m horizon may reflect rapid deposition rate at that time, or that the environment was not suitable for storing organic substances such as pollen.

Three samples were taken from KKC-13 at 6.6, 10.6 and 14.8 m. However, horizons 6.6 m and 10.6 m showed no pollen, which indicated a faster deposition rate at that time or a sedimentary environment that was not suitable for storing organic matters such as pollen (Figure 7). The sample from 14.8 m yielded a pollen concentration of 3089 pollen spores/cm<sup>3</sup>. The sample showed an AP content of 23% of low-altitude forest species such as *Castanopsis* (11%). Wetland pollen was dominated by Cyperaceae (69%) and many organic debris.

The pollen analyses showed slightly different conditions in the three cores. While all three cores indicate a wetland environment and adjacent low-altitude forests, KKC-09 represented higher energy conditions with frequent landslide and fluvial deposits and KKC-01 revealed sporadic local landslide occurrences indicated at depths 10.8 and 15.8 m.

## 5.2 | Foraminifera results

In the six samples from the KKC-01 core, the most foraminifera individuals appeared at 13.2 and 7.2 m (Figure 8). Only two individuals were found at 18.6 m and two at 15.8 m horizons, though the

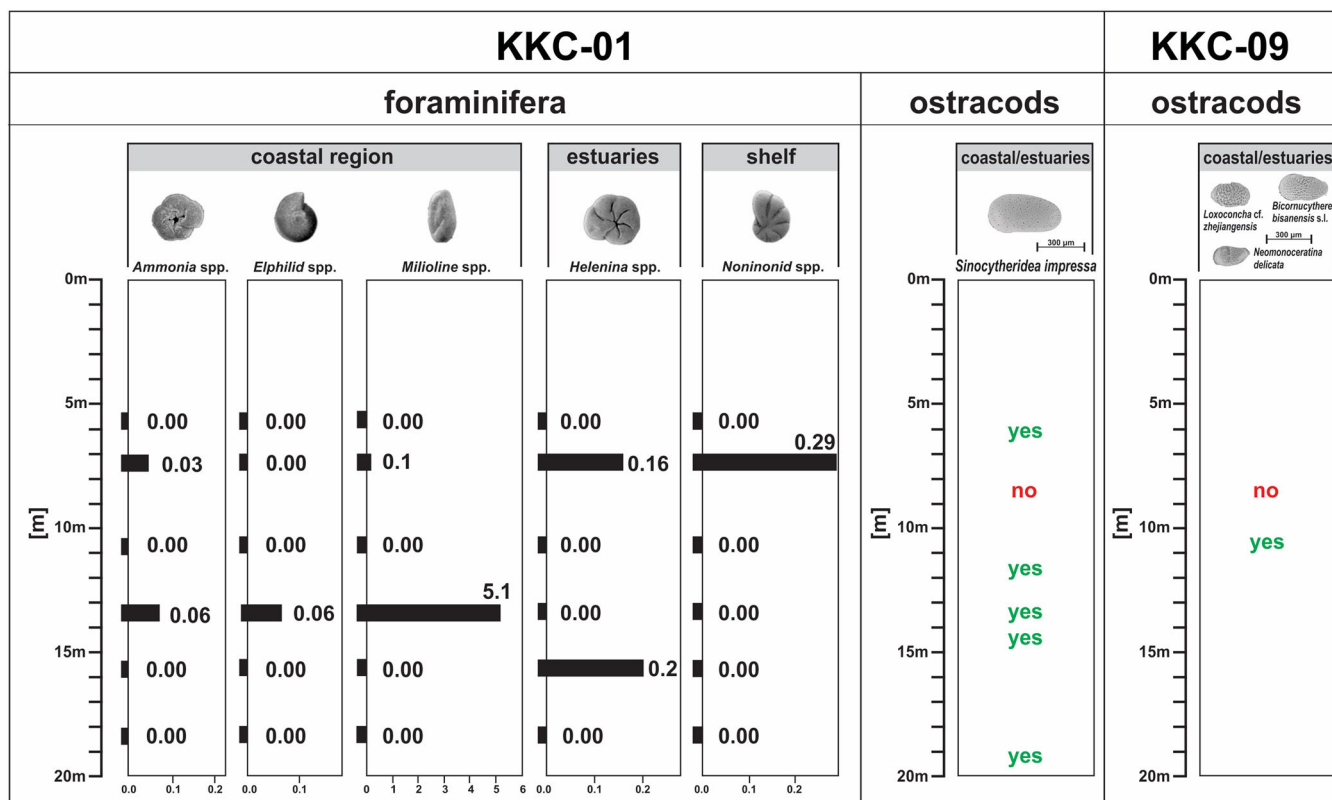


**FIGURE 8** Foraminifera and ostracod data from cores KKC-01 and KKC-09. The foraminifera individuals show environment characterized by close to the coast and decreased salinity waters. Ostracod analyses confirm the same environment. In the core KKC-09 the foraminifera were found broken in a chaotic form. No foraminifera and ostracod individuals were found in core KKC-13

individuals found at 18.6 m were classified as unknown. The 15.8-m horizon showed two individuals of *Helenina* spp., which represents a brackish environment. The 13.2 m interval was dominated by *Milioline* spp., also contained one individual of the genus *Ammonia* spp. and one of *Elphidium advenum*. The horizon 7.2 m contained a small amount of *Helenina* spp. and *Nonionid* spp. No foraminifera were found at depths of 10.8 and 5.8 m.

The abundance and species differences such as *Helenina* spp., *Milioline* spp. or *Nonionid* spp. reflect the change in salinity in the area. *Helenina* prefers a brackish water environment, while *Milioline* spp. can adapt to a high salinity environment (e.g., hypersaline lagoon). Changes in salinity may be related to sea level rise and drop which resulted in the estuary closure at different times.

In the three samples of KKC-09 only one horizon at 10.8 m showed abundant foraminifera, however in a very chaotic and dispersed form (Figure 8). Also, 'fresh' *Amphistegina* sp. as well as *Rectobolivina* sp. foraminifera belonging to a farther offshore planktonic environment community were found. These far-shore communities with accompanying large numbers of reworked Miocene fossils suggest strong wave events that brought material from distant areas. Also, the eroded material suggests that it was brought by increased energy waves related either to storms or deeper water environments at the time the sediment was deposited.

No foraminifera individuals were found in the entire core of KKC-13.

### 5.3 | Ostracods results

At least five ostracod species were identified from six horizons of the KKC-01 core (Figure 8). However, the most abundant ostracods are

represented by *Sinocytheridea impressa*, occupying more than 90% of the total individuals in each sample in all depths: 6.3, 11.8, 13.38, 14.5 and 19.17 m. The appearance of *S. impressa* in mud sediments implies that the layer represents brackish waters in the vicinity of a river mouth or estuary at a water depth of less than 20 m (e.g., Wang & Zhao, 1985). No ostracod was found at a depth of 8.5 m.

As in KKC-01, the KKC-09 showed over 90% of the ostracod individuals that belong to *S. impressa* (Figure 8). In addition, *Bicornucythere bisanensis* s.l., *Neomonoceratina delicata* and *Loxococoncha* sp. were subdominant in the sample at a core depth of 10.5 m. Thin mud sediments intercalated within fluvial channel deposits contain a few inner bay ostracod taxa such as *B. bisanensis* and *Neomonoceratina delicata*. This suggests that the coastline was located landward from the region of KKC-09 during the depositional period. Also, a relative higher sea-level might have occurred at this period.

Similar to foraminifera, no ostracods were found in the entire core of KKC-13. The lack of marine organisms in the core KKC-13 can be interpreted to indicate freshwater lacustrine deposits, since it is unlikely to show evidence of a complete absence of any foraminifera or ostracod individuals in the marine deposits, even if these deposits are highly deformed or dispersed. These observations significantly differ from the brackish environment of the lower reaches of the Gangkou basin at the locations of KKC-01 and KKC-09.

### 5.4 | Fieldwork and digital elevation model-based surveys

The geological mapping coupled with DEM and surface deformation pattern provides information that further aids to frame the

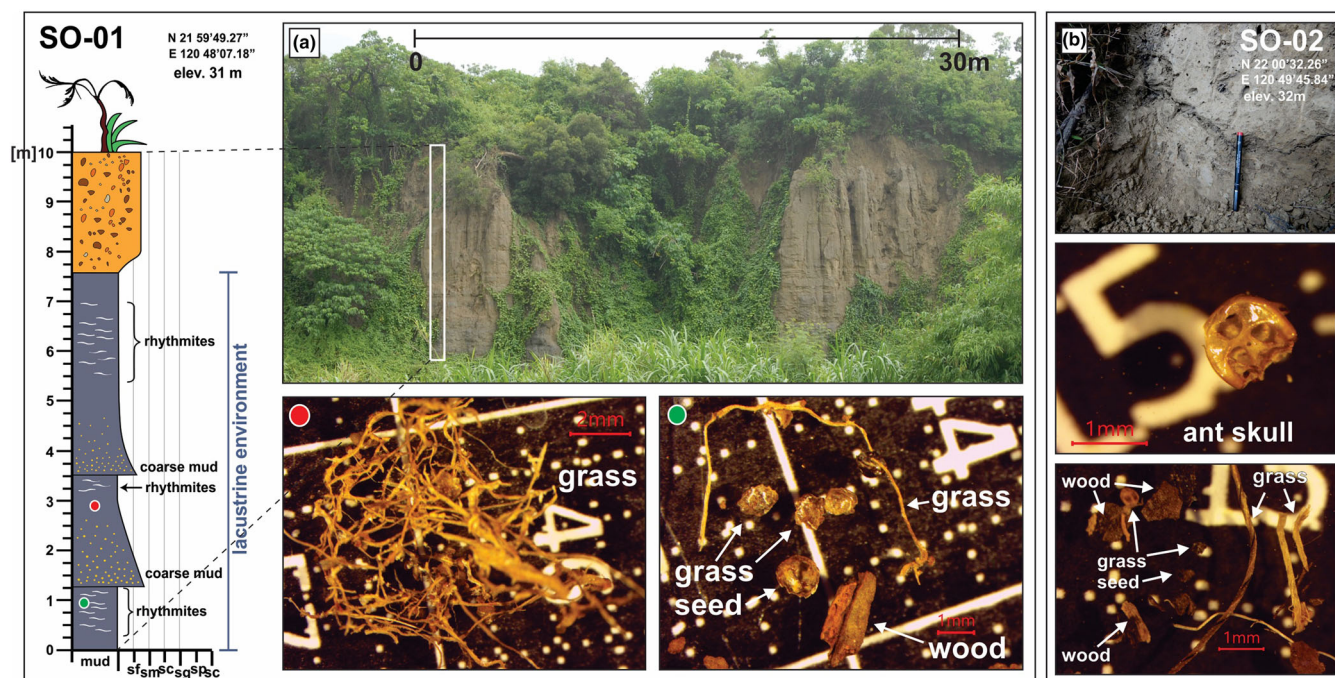


**FIGURE 9** (a) Large outcrop (SO-01) of the dark lacustrine sediment in the central part of the Gangkou basin which thickness is used for the digital elevation model (DEM) simulation to visualize the lake area (see Figures 5 and 10). The optical microscopic analyses show abundance of grass, seeds and wood as shown in the microscopic view. The presence of thin sandy layers (rhythmites) in thick mud indicates low energy sedimentary-lacustrine conditions. No foraminifera or diatoms were found. (b) A 1 m deep trench (SO-02) in the central part of the Gangkou basin (see the location in Figures 5 and 10). The soil profile exposed the same dark mud lacustrine deposits with large abundance of organic matters as land grass, seeds and wood. At the depth of 0.8 m we have found an ant's skull that might indicate the closure of the lake coast

paleoenvironment of the Hengchun Peninsula. The low relief area in the central part of the peninsula (Figure 4a) can be traced to the north into the upstream of the Sizhong basin where it is a relict landscape – Mudan Ponds (Giletycz et al., 2015; Yang et al., 2011). The fieldwork focused on the low-relief area of Gangkou basin with the aim to locate records corresponding to the relict landscape of Mudan Ponds.

A key outcrop (SO-01) is located in the south-western area of the basin (Figure 5). This outcrop is comprised of two sequences of mudstone with a small sand component (~10%) at their base and rhythmites at their tops (Figure 9a). A possible third, lower sequence is found as rhythmites at the base of the outcrop. The mudstone is uncomfortably overlain by highly weathered soil and pebbles of

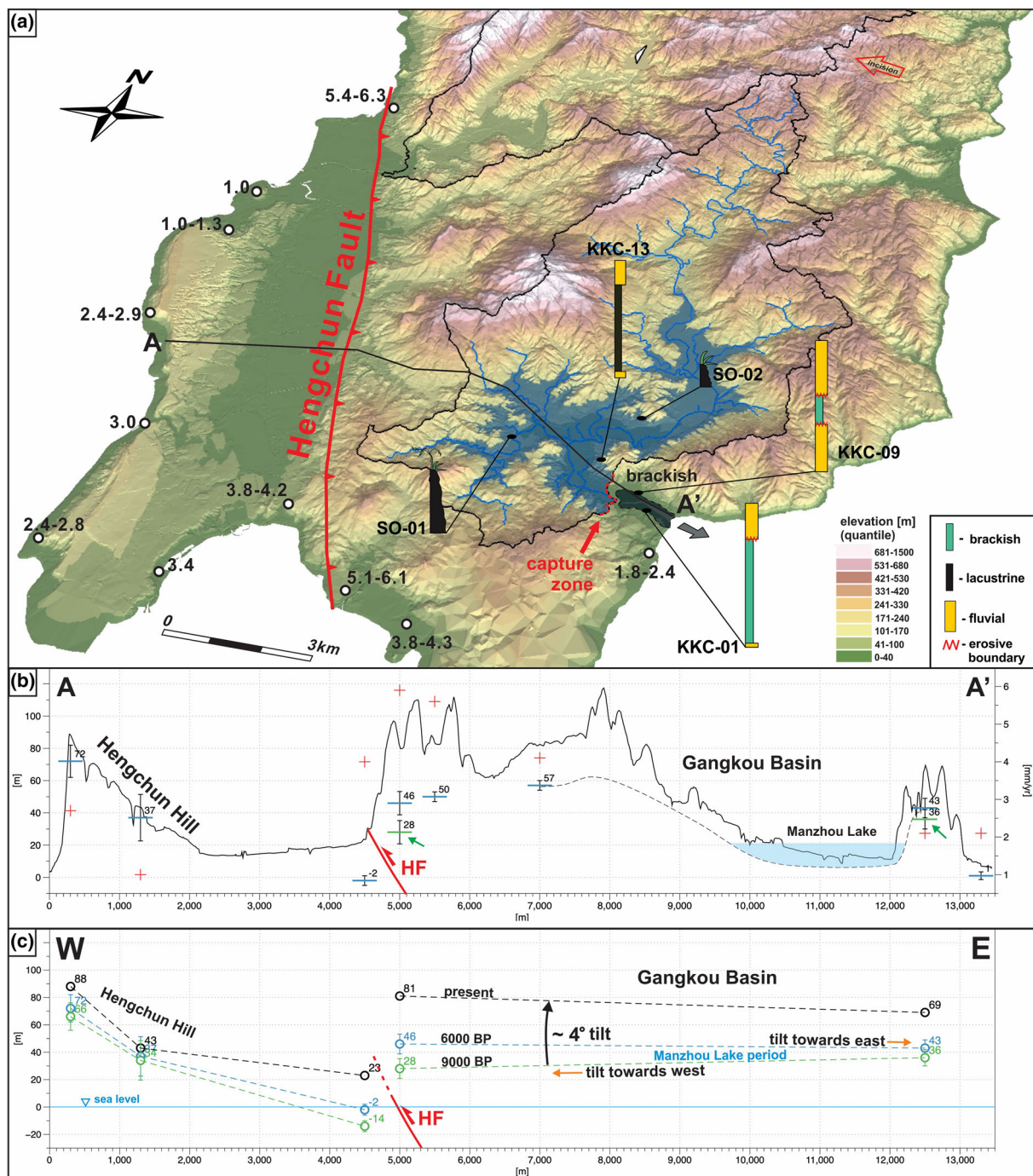


**FIGURE 10** (a) Three-dimensional (3D) image of southern Hengchun Peninsula and a former Manzhou Lake in the present Gangkou basin with locations of three drill sites and two outcrops discussed in this study. The capture zone is indicated by the red-dashed line. The numbers represent uplift rates based on radiocarbon dating of coral terraces (Chen & Huang, 1975; Chen et al., 2014; Liew & Lin, 1987). (b) Topographic profile across southern Hengchun Peninsula and the Manzhou Lake (the constraints on the lake elevations are explained in Section 6.1), the plot's right label indicates uplift rates in mm/yr (also red crosses), left label indicate elevation blue dashes and values show elevations at the beginning of the lake existence (9000 yr BP) in correlation to present topography elevations. (c) Surface tilt based on uplift rates along the topographic profile. The values on the plot show the elevation in each topographic period (mm). The data clearly shows influence of the Hengchun Fault. Since the first records of lacustrine deposits (9000 yr BP) the surface of the hanging wall tilted about 4° eastward. Note, at the time of the lake creation the surface was dipping westward. During the Manzhou Lake stage, the surface was nearly balanced out, when about 6000 yr BP the surface inclined eastward. It could also exert influence on the capture point at the eastern brackish waters. Note also, to the west, the lagoon elevations below the sea level before 6000 yr BP

sandstone. The rhythmites evidence a low energy depositional environment. The optical microscopic studies on the large abundance of organic matter revealed a number of freshwater indicators, such as grass seeds, freshwater pollen (*Cyperaceae*), twigs or small branches (Figure 9a). No diatoms or foraminifera were found, although several freshwater gastropods (*Amnicola* genus) appear in the lower part of the outcrop.

The outcropping mudstone in SO-01 correlates with the dark lacustrine mud described in core KKC-13. We therefore, correlated these two to perform 'flood simulation' on 5 m DEM by adopting the highest elevation of the mud deposit from the outcrop SO-01 and KKC-01 to visualize a potential reach and size of the lake. For this simulation, we used a present-day DEM since there is no sufficient data to reconstruct 3D topography of the southern Hengchun Peninsula 9000 yr BP. Consequently, the results are approximate. The results suggest that a waterbody covered much of the lower and central parts of the Gangkou basin, with an area reaching about 20 to 22 km<sup>2</sup> (Figure 10a). The 'flood simulation' results helped us to trace a lake coast zone to survey beach characteristics where we located and performed a 1-m deep trench (SO-02) in the northern areas of the basin (Figures 5 and 10a). The soil profile showed similar dark mud lacustrine deposits with a large abundance of organic matter, such as grass pollen (*Cyperaceae*) as well as wood pieces and grass roots (Figure 9b). However, it was not possible to survey characteristics of the beach due to very dense vegetation and extensive farming in the area.

A DEM was also used to survey a deformation pattern of the peninsula's surface. Based on radiocarbon dating of the marine terraces (Chen & Liu, 1993; Chen et al., 2014; Liew & Lin, 1987), long-term uplift rates reveal that active tectonic deformation might influence the evolution of the Manzhou Lake. The western coast of the Hengchun Peninsula represents a footwall of the Hengchun Fault with uplift rates from 1 to 4 mm/yr with slight increase of the uplifts towards the south (Figure 10a). The hanging wall however, shows much higher uplift rates between 5 and 6.3 mm/yr (Figure 10b), though local radiocarbon dating indicates even 7.5 mm/yr (Chen et al., 2014). Recent studies suggest that the Hengchun Fault is still active with a creeping character (Chen et al., 2005, 2014; Giletycz et al., 2017). The eastern coast of the Hengchun Peninsula shows distinctive lower uplift rates from 1.8 to 2.4 mm/yr. As a result, the east-west profile of the peninsula demonstrates that the peninsula's surface tilts towards the east (Figure 10c). This also includes the Gangkou basin and the area of the former Manzhou Lake found in the deposits in KKC-12, SO-01 and SO-02.

## 6 | DISCUSSION

### 6.1 | Lake area estimations

The data from KKC-13 combined with the field mapping draws an image of a vast freshwater lake in the central and lower parts of the present Gangkou basin. The large outcrop in the inner basin (SO-01) shows lacustrine deposits as a relict mark of this lake (Figure 9a). It exposes 8-m thick dark mud with typical rhythmites. Also, a trench (SO-02) conducted in the central area of the Gangkou basin exposes dark and well-sorted fine mud (Figure 9b) that is characteristic to a calm sedimentary environment prevalent in lacustrine conditions and

indicates the same paleoenvironment of an enclosed freshwater body was found in SO-01 and core KKC-13. A correlation of these three findings gave a basis for a flood simulation model in the Gangkou basin. This was achieved by using a 5 m DEM which raised the water level in the basin to the highest point of the lacustrine sediments found in the outcrop SO-01. Based on the earlier data, the flood simulation draws a large lake with an approximate area of 20 to 22 km<sup>2</sup> (Figure 10a).

### 6.2 | Lake age estimations

The radiocarbon dating of the lacustrine sediments shows the appearance and extinction of the lake within the Holocene. Due to the lack of an adequate material at the lower and upper parts of the lacustrine deposits, we were not able to sample exactly or close to lithological boundaries, however the results from all the cores and their correlation indicate the age of the lake to be in the time-gap between roughly 9000 yr BP to about 6000 yr BP, which we accept as a close approximation. In KKC-13, at the depths 10.15 m the material yields 12,340 yr BP ( $\pm 40$  yr BP), which is about 4500 years older than material at the lower boundary of the lacustrine deposits at 14.68 m – 8710 ( $\pm 30$ ) yr BP (Figure 6). The anomalous older age at the depth 10.15 m core corresponds to a coarser material in the lacustrine deposits. It is our opinion that this level represents an episode such as a local landslide or increased sediment discharge by fluvial processes due to extreme events such as typhoons or earthquakes. As a result, material from an area of the older formations was eroded elsewhere and brought to the lake.

### 6.3 | Sea/lake paleoenvironment evolution

The cores KKC-01 and KKC-09 located in the present Gangkou estuary revealed a different paleoenvironment than that found in the KKC-13 and fieldwork. The large abundance of *S. impressa* ostracods (over 90% of total individuals) and foraminifera as *Milioline* spp., *Helenina* spp., in KKC-01 and KKC-09 suggest a shallow environment of decreased salinity (< 20 m) (Figures 10a and 11) close to the coast (Tanaka et al., 2019; Whatley & Zhao, 1987). This evidence implies that the former Gangkou estuary was characterized by brackish waters or a lagoon. In that case, the Gangkou brackish waters were likely separated from the lake by a drainage divide (Figures 10 and 11). Pollen data suggests that this area was also surrounded by low-altitude forests affected by periodic landslides or fluvial deposits from surrounding slopes, which is furthermore supported by the presence of pollen in a lithological column KKC-09. This indicates increased topographic local relief in the vicinity of the brackish waters. Based on DEM and the altitudes of the cores corrected by uplift rates, the brackish waters could extend 2-to-3 km inland with its coast near the eastern limb of the bifurcated drainage divide (Figures 10a and 11).

In core KKC-09, at the depth of 10.5 m the horizon showed a change of the environment. The presence of several inner bay ostracods (*B. bisanensis* and *Neomonocerotina delicata*) indicates deeper-water conditions and implies that the coastline likely moved landward. Also, Miocene *Amphistegina* spp., *Rectobolivina* spp., and planktonic foraminifera found at 10.8 m indicate a distant environment

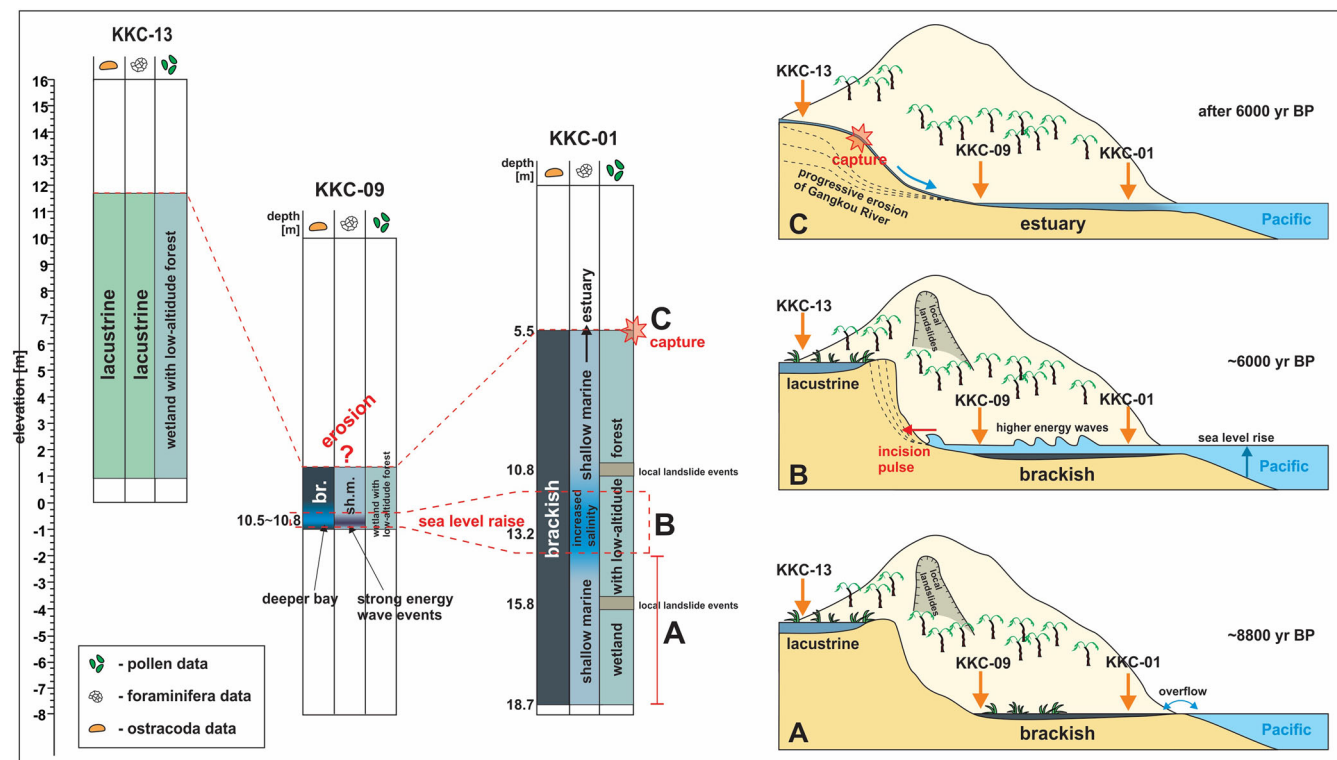


**FIGURE 11** The evolutionary model of the brackish waters at the eastern coast of the Hengchun Peninsula that due to the capture event were turned into the present drainage basin estuary (A). The integrated analysis from ostracodes, foraminifera and pollen analyses permitted to reconstruct phases that led to the lake extinction. The KKC-09 and KKC-01 cores showed around 6000 yr BP increased water energy and salinity that could be explained by a sea level rise (Chiba et al., 2016; Lüthgens et al., 2018; Nakada et al., 1991; Okuno et al., 2014). At that time, the coast line moved to the landward side of the brackish water and triggered the incision pulse (B). Several indicators from foraminifera studies revealed local landslides suggesting that the area also represented more active surface erosional processes. The continued incision finally led to the capture that drained the Manzhou Lake into the Pacific (C)

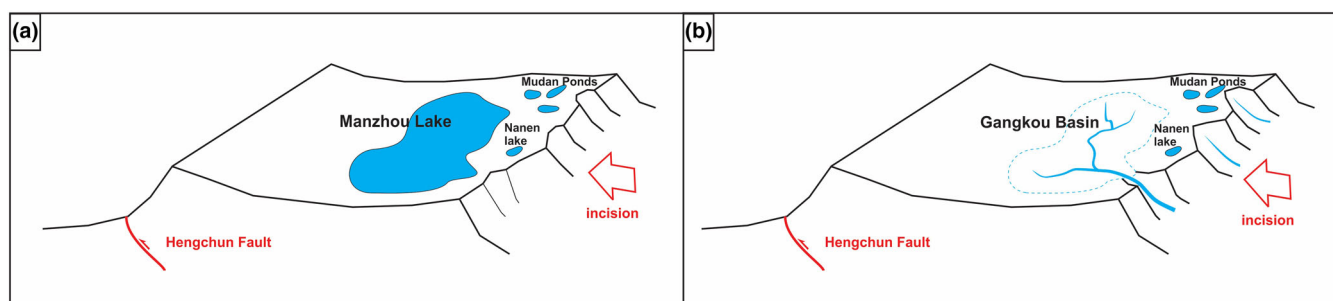


**FIGURE 12** Model showing transformation of the Manzhou Lake into Gangkou Basin through the brackish waters – present Gangkou estuary. Relict lakes and ponds (Mudan and Nanen) still remain at the north-eastern flank of the peninsula

community that implies increased depth of the brackish waters. In this horizon, an accompanying large number of displaced foraminifera fossils also suggests stronger waves. The sea level change was also confirmed by foraminifera data (*Nonionid* spp.) in KKC-01 at 7.2 m, which characterizes a higher salinity environment. The radiocarbon dating yields this event at roughly 6000 BP and correlates to the increase of a sea-level that occurred at this time (Figure 6) (also Chiba et al., 2016; Nakada et al., 1991; Okuno et al., 2014). This indicates that at about 6000 yr BP, the brackish waters experienced a rise in the level of seawater with a coastline migrating westwards. Based on DEM, the coast could move up to 100 m landwards (Figure 11b). We

suggest that this led to an incision pulse of the backslope (Figure 11b) which also affected surrounding slopes that resulted in frequent landslides what is found by increased low-altitude forest pollen species (*Castanopsis*) in cores KKC-01 and MMC-09. This incision propagated westward in the same manner as the presently reported captures along the eastern coast of the Hengchun Peninsula (Giletycz et al., 2015) (Figure 3b). As a consequence, the progressive incision led to capture of the eastern drainage divide and drained the Manzhou Lake into the Pacific (Figures 11c and 12). The rise of the sea level coincides with the age of the youngest lacustrine records found in KKC-13, therefore, the time of the extermination of the lake.

This event turned the lake from a temporarily preserved depositional domain into a fluvial system – the Gangkou basin (Figure 3).

The elevations of brackish and lacustrine sediments in KKC-01, KKC-09 and KKC-13, respectively, show that the water level difference between lacustrine and brackish paleoenvironment was a minimum of 5 m. Both, KKC-01 and KKC-09 show erosional contact above the brackish sediments (Figure 6) that indicates the release of a large amount of water. No erosional contact with the lacustrine sediments KKC-13 was found. It can be concluded that a water gap at the present Gangkou estuary represents a relict area of the capture point that drained the Manzhou Lake into the Pacific (Figure 5).

## 6.4 | Morphologic model

Based on radiocarbon dating of marine terraces in the southern Hengchun Peninsula (Cheng & Huang, 1975; Chen et al., 2014; Liew & Lin, 1987), the uplift rates show that high reliefs at the western flank of the peninsula have been built by a continuous uplift of the Hengchun thrust fault (Figures 10b and 4) (Chen et al., 2005; Giletycz et al., 2017). The uplift rates of the hanging wall demonstrate 5 to 6.3 mm/yr while the footwall 1.0 to 4.2 mm/yr. The continuous displacement of the hanging wall consequently raised the western Hengchun Peninsula to 1000 m above sea level (Lilong Range). At the eastern coast, however, the radiocarbon dating indicates much lower uplift rates of 1.8 to 2.4 mm/yr. A correlation of the uplift rates across the peninsula and its topography reveals that its surface is under an eastward tilt (Figure 10c). By coupling this trend with the age of the Manzhou Lake, we believe that since 9000 yr BP (see Section 6.2), the area of the Gangkou basin tilted 4° to 5° eastwards (Figure 10c). In such a case, the rates of the tilt suggest that at the initial stage of the lake at about 9000 BP, the topography of the Gangkou basin was dipping westward. Then, during the lake's existence (between 9000- and ~6000-yr BP) the gradient of the Gangkou basin was roughly horizontal, and after 6000 yr BP it started to incline to the east. This might suggest that this topographic tilt played a pivotal role in the extermination of the lake as well as in a recent landscape rearrangement.

Our study shows that by linking different environment records in correlation with tectonic activity, we are able to reconstruct evolutionary models of landscape rearrangement. The results show that the freshwater Manzhou Lake adopted the enclosed topographic low-relief in the present Gangkou basin. The low-relief topography (< 250 m) (Figure 4), however, extends northward into another – Sizhong basin, where wetlands (Mudan Ponds and Nanren Lake) are still preserved as a relict landscape of a former paleoenvironment (Giletycz et al., 2015) (Figure 12). The Mudan Ponds and Nanren Lake are being progressively captured by advanced incision from the east which is consuming this area in favour of the eastern basins as described earlier in this article (Figure 3b). This survey also suggests that there might have been more lakes and ponds in an earlier stage of the landscape development, though at present we have not found any indication that could be related to erosion or dense vegetation in this area.

A submarine topography after emergence above the sea level is subjected to ample processes that transform its surface to a juvenile fluvial system that tends to create ephemeral landforms including lakelands. While lakes can be formed by tectonic, volcanic, or riverine activity, as well as landslides, wind erosion, etc. (Hutchinson, 1957),

here, we point out that newly emerged topography can also lead to lake formation.

## 7 | CONCLUSIONS

We have pointed out that in the southern Taiwan the landscape reorganization of one geomorphic system can build and remove landforms in a very short period and still have a major impact on its topography. One of the major findings in this study is a reconstruction of the freshwater lake that adopted the enclosed topographic depressions and correlates to the preserved relict landscapes of Mudan Ponds and Nanren Lake. The radiocarbon dating of lacustrine sediments reveals that the appearance and extinction of the lake took place within the Holocene, which also might indicate an approximate time of the emergence of the peninsula above a sea level. A new geomorphic system temporarily preserved depositional domain, however an initiation incision from the east and progressive captures of the westwards draining systems led to extinction of the lake and the transforming of the system into a drainage basin (Gangkou basin) therefore resulting in a sediment outflux domain.

The asymmetrical uplift rates of the Hengchun Peninsula show that the surface is under fast processes of a landscape rearrangement and a few important phases of the paleoenvironment change have been pointed out. Firstly, advancing incision rates from the eastward draining basins, captures drainage basins and wetlands at the western side of the drainage divide. This causes rapid changes of the fluvial system but also progressively migrates the drainage divide towards the central part of the peninsula. Secondly, the activity of the Hengchun Fault shows that the western flank of the peninsula has about 3 mm/yr higher uplift rates than the eastern flank. This leads to a surface tilt towards the east. Within the last 10,000 years, during the lake's existence, the surface underwent about 4° tilt shifting the peninsula's surface causing a dip from west to east. This results in higher local-relief is being built at the western flank of the peninsula. The coupling of these two conclusions indicates that the present configuration of the peninsula's geomorphic system is still under advancing reorganization and its progress in fast rates removes relict landscape preserved in the northern area of the Sizhong basin: the low-relief Mudan Ponds.

## ACKNOWLEDGEMENTS

This study is funded by the Ministry of Science and Technology under the grant MOST 108-2116-M-008-002 to A.T. Lin. The KKC cores are provided by Sinotech Engineering Consultants, Ltd.

The authors would like to send their appreciation to Mr Ryuji Kenmotsu (Shinshu University, Japan) for the essential support in ostracoda processing. The authors would like to thank the Editor Stuart Lane and two anonymous Reviewers for the vital comments and suggestions over the manuscript. Also, the authors want to address special thanks to Dennis Brown for indispensable comments and advice during the shaping of this article and Clyde van Zyl for the English editorial corrections.

## CONFLICT OF INTEREST

The authors declare that no conflict of interest exists over the manuscript.

## DATA AVAILABILITY STATEMENT

The repository data folder is at:

[https://figshare.com/articles/dataset/data\\_giletycz\\_et\\_al\\_zip/12965276](https://figshare.com/articles/dataset/data_giletycz_et_al_zip/12965276)

Data openly available in a public repository that does not issue DOIs.

## ORCID

Slawomir Jack Giletycz  <https://orcid.org/0000-0002-0491-2221>

Chih-Wei Chien  <https://orcid.org/0000-0003-0790-2296>

## REFERENCES

- Anderson, R.S., Jiménez-Moreno, G., Ager, T. & Porinchu, D. (2014) High-elevation paleoenvironmental change during MIS 6–4 in the central Rockies of Colorado as determined from pollen analysis. *Quaternary Research*, 82(3), 542–552. <https://doi.org/10.1016/j.yqres.2014.03.005>
- Attal, M., Tucker, G.E., Whittaker, A.C., Cowie, P.A. & Roberts, G.P. (2008) Modeling fluvial incision and transient landscape evolution: Influence of dynamic channel adjustment. *Journal of Geophysical Research*, 113, F03013.
- Chen, W.-S., Lee, W.-C., Hunag, N.-W., Yen, I.-C., Yang, C.-C., Yang, H.-C., et al. (2005) Characteristics of accretionary prism of Hengchun Peninsula, southern Taiwan: Holocene activity of the Hengchun Fault. *Western Pacific Earth Sciences*, 5, 129–154.
- Chen, W.-S., Matta, N.-H., Chu, Y.-K., Yu, N.-T. & Yang, H.-C. (2014) Holocene activity of the Hengchun Fault in the southern Taiwan: Evidenced from the radiometric dating of uplifted coral reef terraces. *Special Issue of the Central Geological Survey of the Ministry of Economic Affairs*, 28, 1–18.
- Chen, Y.-G. & Liu, T.-K. (1993) Holocene radiocarbon dates in Hengchun Peninsula and their neotectonic implications. *Journal of the Geological Society of China*, 36(4), 457–479.
- Cheng, Y.-M. & Huang, C.-Y. (1975) Biostratigraphic study in the west Hengchun Hill. *Acta Geologica Tawanica*, 18, 49–59.
- Chiba, T., Sugihara, S., Matsushima, Y., Arai, Y. & Endo, E. (2016) Reconstruction of Holocene relative sea-level change and residual uplift in the Lake Inba area, Japan. *Palaeogeography Palaeoclimatology Palaeoecology*, 441, 982–996. <https://doi.org/10.1016/j.palaeo.2015.10.042>
- Dadson, J.D., Hovius, N., Chen, H., Dade, W.B., Hsieh, M.-L., Willet, S.D., et al. (2003) Links between erosion, runoff, variability and seismicity on the Taiwan orogen. *Nature*, 426(6967), 648–651. <https://doi.org/10.1038/nature02150>
- Dahlquist, M.P., West, A.J. & Li, G. (2018) Landslide-driven drainage divide migration. *Geology*, 46(5), 403–406. <https://doi.org/10.1130/G39916.1>
- Giletycz, S.J., Chang, C.-P., Lin, A.T.-S., Ching, K.-E. & Shyu, J.B.H. (2017) Improved alignment of the Hengchun Fault (southern Taiwan) based on fieldwork, structure-from-motion, shallow drilling, and levelling data. *Tectonophysics*, 721, 435–447. <https://doi.org/10.1016/j.tecto.2017.10.018>
- Giletycz, S.J., Lin, A.T.-S., Chang, C.-P. & Shyu, J.B.H. (2019) Relicts of mud diapirism of the emerged wedge-top as an indicator of gas hydrate destabilization in the Manila Accretionary prism in the southern Taiwan (Hengchun Peninsula). *Geomorphology*, 336, 1–17. <https://doi.org/10.1016/j.geomorph.2019.03.022>
- Giletycz, S.J., Loget, N., Chang, C.-P. & Mouthereau, F. (2015) Transient fluvial landscape and preservation of low-relief terrains in an emerging orogen: Example from Hengchun Peninsula, Taiwan. *Geomorphology*, 231, 169–181. <https://doi.org/10.1016/j.geomorph.2014.11.026>
- Hong, Y., Yasuhara, M., Iwatani, H. & Mamo, B. (2019) Baseline for ostracod-based northwestern Pacific and Indo-Pacific shallow-marine paleoenvironmental reconstructions: ecological modeling of species distributions. *Biogeosciences*, 16(2), 585–604. <https://doi.org/10.5194/bg-16-585-2019>
- Huang, C.-Y., Wu, W.-Y., Chang, C.-P., Tsao, S., Yuan, P.B., Lin, C.-W. & Xia, K.-Y. (1997) Tectonic evolution of accretionary prism in the arc-continent collision terrane of Taiwan. *Tectonophysics*, 281(1–2), 31–51. [https://doi.org/10.1016/S0040-1951\(97\)00157-1](https://doi.org/10.1016/S0040-1951(97)00157-1)
- Huang, C.-Y., Yuan, P.B. & Tsao, S.-J. (2006) Temporal and spatial records of active arc-continent collision in Taiwan: A synthesis. *GSA Bulletin*, 118(3–4), 274–288. <https://doi.org/10.1130/B25527.1>
- Hugget, R.J. (1988) Dissipative systems: Implications for geomorphology. *Earth Surface Processes and Landforms*, 13(1), 45–49. <https://doi.org/10.1002/esp.3290130107>
- Hutchinson, G. (1957) *A treatise on limnology: Vol. I. Geography, physics and chemistry*. New York: Wiley.
- Liew, P.-M. & Lin, C.-F. (1987) Holocene tectonic activity of the Hengchun Peninsula as evidenced by the deformation of marine terraces. *Memoir of Geological Society of China*, 9, 241–259.
- Lin, A.T., Yao, B., Hsu, S.-K., Liu, C.-S. & Huang, C.-Y. (2009) Tectonic features of the incipient arc-continent collision zone of Taiwan: Implications for seismicity. *Tectonophysics*, 479(1–2), 28–42. <https://doi.org/10.1016/j.tecto.2008.11.004>
- Liu, T.K., Hsieh, S., Chen, Y.-G. & Chen, W.-S. (2001) Thermo-kinematic evolution of the Taiwan oblique-collision mountain belt as revealed by zircon fission track dating. *Earth and Planetary Science Letters*, 186(1), 45–56. [https://doi.org/10.1016/S0012-821X\(01\)00232-1](https://doi.org/10.1016/S0012-821X(01)00232-1)
- Lüthgens, L.-D., Ho, N., Clemenz, J.-H., Chen, C.-H., Jen, J.-Y.Y. & Chyi, S.-J. (2018) The Holocene paleo-environmental history of the Gangkou River estuary, Hengchun Peninsula, Taiwan. *Terrestrial, Atmospheric and Oceanic Sciences*, 29(5), 547–576. <https://doi.org/10.3319/TAO.2018.05.07.01>
- Nakada, M., Yonekura, N. & Lambeck, K. (1991) Late Pleistocene and Holocene sea-level changes in Japan: Implications for tectonic histories and mantle rheology. *Palaeogeography Palaeoclimatology Palaeoecology*, 85(1–2), 107–122. [https://doi.org/10.1016/0031-0182\(91\)90028-P](https://doi.org/10.1016/0031-0182(91)90028-P)
- Okuno, J., Nakada, M., Ishii, M. & Miura, H. (2014) Vertical tectonic crustal movements along the Japanese coastlines inferred from late Quaternary and recent relative sea-level changes. *Quaternary Science Reviews*, 91, 42–61. <https://doi.org/10.1016/j.quascirev.2014.03.010>
- Ramsey, L.A. (2006) Topographic evolution of emerging mountain belts, *PhD Thesis*.
- Ramsey, L.A., Walker, R.T. & Jackson, J. (2007) Geomorphic constraints on the active tectonics of southern Taiwan. *Geophysical Journal International*, 170(3), 1357–1372.
- Stolar, D.B., Willet, S.D. & Montgomery, D.R. (2007) Characterization of topographic steady state in Taiwan. *Earth and Planetary Science Letters*, 261, 421–431.
- Tanaka, G., Henmi, Y., Masuda, T., Moriwaki, H., Komatsu, T., Zhou, B. & Ikeya, N. (2019) Recent ostracod distribution in western Kyushu, Japan, related to the migration of Chinese continental faunal elements. *Marine Micropaleontology*, 146, 1–38.
- Wang, L.C., Behling, H., Kao, S.-J., Li, H.-C., Selvaraj, K., Hsieh, M.-L. & Chang, Y.-P. (2015) Late Holocene environment of subalpine north-eastern Taiwan from pollen and diatom analysis of lake sediments. *Journal of Asian Earth Sciences*, 114, 447–456. <https://doi.org/10.1016/j.jseaes.2015.03.037>
- Wang, L.-C., Tang, Z.-W., Chen, H.-F., Li, H.-C., Shiao, L.-J., Huang, J.-J.S., et al. (2019) Late Holocene vegetation, climate, and natural disturbance records from an alpine pond in central Taiwan. *Quaternary International*, 528, 63–72. <https://doi.org/10.1016/j.quaint.2019.03.005>
- Wang, P. & Zhao, Q. (1985) Ostracod distribution in bottom sediments of the East China Sea. In: Wang, P. (Ed.) *Marine Micropaleontology of China*. Beijing: China Ocean Press, pp. 70–92 (in Chinese).
- Whatley, R. & Zhao, Q. (1987) A revision of Brady's 1869 study of the Ostracoda of Hong Kong. *Journal of Micropaleontology*, 6, 21–29.
- Whipple, K.X. (2001) Fluvial landscape response time: how plausible is steady-state denudation? *American Journal of Science*, 301, 313–325.

- Whipple, K.X., Forte, A.M., DiBiase, R.A., Gasparini, N.M. & Ouimet, W. B. (2016) Timescales of landscape response to divide migration and drainage capture: Implications for the role of divide mobility in landscape evolution. *JGR Earth Surface*, 122, 248–273.
- Yang, T.-N., Lee, T.-Q., Meyers, P.A., Song, S.-R., Kao, S.-J., Löwemark, L. & Chen, R.-F. (2011) Variations in monsoonal rainfall over the last 21 kyr inferred from sedimentary organic matter in Tung-Yuan Pond, southern Taiwan. *Quaternary Science Reviews*, 30 (23–24), 3413–3422. <https://doi.org/10.1016/j.quascirev.2011.08.017>
- Zhao, Q. & Wang, P. (1988) Distribution of modern Ostracoda in the shelf seas off China. In: Hanai, T., Ikeya, N. & Ishizaki, K. (Eds.) *Evolutionary*

*Biology of Ostracoda: Its Fundamentals and Applications*. Tokyo: Kodansha, pp. 805–821.

**How to cite this article:** Giletycz, S.J., Lin, A.T.-S., Yamada, K., Wang, L.-C., Chien, C.-W., Lou, J.-Y. et al. (2021) Ephemeral landform development following rapid coastal uplift in the southern orogen of Taiwan. *Earth Surface Processes and Landforms*, 1–16. Available from: <https://doi.org/10.1002/esp.5183>